Combined oxidative and non-oxidative dehydrogenation of *n*-butane over VO_X species supported on HMS

M. Setnička*, P. Čičmanec, E. Tvarůžková, R. Bulánek

Department of Physical Chemistry, University of Pardubice, Studentská 573, CZ 532 10 Pardubice, Czech Republic
**corresponding author: Michal.Setnicka@upce.cz*

Abstract

The combination of oxidative and non-oxidative dehydrogenation of *n*-butane as an attractive possibility for production of C_4 olefins was studied over VO_X based catalyst. Long-term activity and selectivity to desired products could be achieved over the catalysts with well dispersed monomeric vanadium oxide species supported on mesoporous silica support.

Keywords: vanadium oxide, oxidative dehydrogenation, lean-oxygen conditions, n-butane, hexagonal mesoporous silica

1 Introduction

The continuously growing demand for C_2-C_4 alkenes, which are the buildings blocks of synthetic rubbers, plastics, automotive fuel components and other valuable chemical products, brings a great challenge for current chemical industry. It stimulates research to improve existing technologies or to develop new ones, which will be able to prepare these materials from cheap and in the future abundant C_2-C_4 alkanes from natural gas [1-3].

There are two direct approaches for alkene production from alkanes, *i.e.* their catalytic non-oxidative (DH) and catalytic oxidative (ODH) dehydrogenation. In the present time, only the catalytic (most often Pt- or Cr-based catalysts supported on alumina [3-5]) dehydrogenation process is carried out on a commercial scale (for example: Houdry Catadiene process, STAR – Phillips Petroleum Co., Oleflex – UOP [5-6]). Although the efficiencies of these processes and catalysts are highly optimized, they have following disadvantages: (i) dehydrogenation of alkanes to alkenes is an equilibrium process between alkane, alkene and hydrogen and the maximum yield of olefins is thus thermodynamically limited, (ii) the number of molecules is higher on the product side and that is why operation at high pressures, which is usually preferred in industry is impossible, (iii) reaction is endothermic (*e.g.*, for *n*-butane $\Delta H°_{298}$ = +125 kJ·mol^{-1} [7]) and for sufficient conversion high temperature is required and reaction needs to supply heat from external source, (iv) use of high temperature leads to alkane cracking and fast coke formation over the catalyst which decreases activity (*e.g.* Cr-Al_2O_3 catalysts used in commercial process require regeneration after a few minutes of operation [8]) [2-3, 5, 9].

The second possible process the oxidative dehydrogenation of alkanes is free of the above mentioned limitations. The formation of water as a very stable product makes this reaction very thermodynamically favourable. In principle a practically complete conversion can be attained even at low temperature ($\Delta H°_{298}$ = –116 kJ·mol^{-1} for *n*-butane [7]) and high

pressures bringing enormous advantages from the economic and process engineering points of view. However, ODH of alkanes still suffers from some problems: (i) low olefin selectivity at industrially relevant conversion due to fast consecutive oxidation of the target olefin to CO_X, (ii) some feed composition ranges can be explosive and that is why it has not been commercialized yet [1-2, 9-10].

The approach that combines DH and ODH in one reactor system could be a good alternative. The under-stoichiometric amount of O_2 (ratio of n-$C_4/O_2 > 10$) suppresses over-oxidation of products to CO_X and the presence of small amount of O_2 helps to burn carbon deposits from the catalysts surface *in situ*. The presence of oxygen also offers improved stability of catalyst in time due to reoxidation of active species. Attempts to combine ODH and DH have already been described in the literature in the past by Tsikoyanni et al. [5, 11] but using two separate reactors with Pt- and Bi-containing catalysts or by Waku et al. [12] in one reactor over Pt-zeolite. Very recently the coupling of these methods was published by Ovsitser *et al.* for ODH/DH propane [2] and *i*-butane [10] over VO_X-species dispersed on silica based support.

Supported vanadium-based catalysts belong to the best performing materials in the ODH of alkanes and they were widely investigated in different types of reactions [13-18]. They were also applied for the classic DH of C_3-C_4 alkane [19-21]. Their employment offers several advantages: low temperature for the activation of C-H bonds of reactants and suitable geometric and electron structure of VO_X. On the other hand vanadium oxide catalysts can not be used in its bulk form (leads to non-selective reactions) but have to be used as the well dispersed VO_X species supported on the suitable support. More details about different structural VO_X-species and properties of vanadium based catalysts can be found in [13, 17, 22-23].

In the present contribution, we report for the first time the production of C_4-olefins through the combination of ODH and DH approach. We tested a set of VO_X-HMS catalysts with different population of vanadium species under different reaction conditions (weight, composition of reaction mixture) to better understand the relationship between vanadium structure on the HMS support and activity in both reactions. To analyze the effect of vanadium concentration on the type of VO_X structure, on dispersion of VO_X and their catalytic activity, the catalysts were characterized by different techniques (SEM, XRF, N_2-adsorption, XRD, DR UV-Vis and H_2-TPR).

2 Experimental

2.1 Preparation of catalysts

Hexagonal mesoporous silica (HMS) was synthesized at ambient conditions according to the procedure reported by Tanev and Pinnavaia [24] by using dodecylamine (DDA, Aldrich) as a neutral structure directing agent and the tetraethylorthosilicate (TEOS, Aldrich) as a silica precursor in the mixture of ethanol and water. More details about these HMS have materials/samples been reported in our papers published previously [13, 22].

The set of synthesized VO_X-HMS catalysts with different amount of vanadium (2-12 wt. % of V) was prepared by wet impregnation method from EtOH solution of vanadyl acetylacetonate. Impregnated samples were dried at 120 °C in air for 14 hours and then calcined at 600 °C in air flow for 8 h (with heating rate of 5 °C/min).

The investigated samples were denoted as S-x where x is the vanadium content expressed as weight percentage.

2.2 Characterization of catalysts

The vanadium content was verified by means of ED XRF by ElvaX (Elvatech, Ukraine) equipped with Pd anode. Samples were measured against the model samples (a mechanical mixture of pure SiO_2 and $NaVO_3$) granulated to grains of the same size as catalysts samples.

The structure and crystallinity of catalysts were probed by scanning electron microscopy (SEM) using JSM-5500LV microscope (JEOL, Japan) and by X-ray diffraction (D8-Advance diffractometer, Bruker AXE, Germany) in the 2θ range of 2-40° with Cu Kα radiation (λ = 1.5406 Å).

Specific surface area and texture of pure HMS and S-12 was measured by means of nitrogen adsorption/desorption in the range of nitrogen relative pressure of 0-0.99 at temperature of liquid nitrogen (77 K) using the ASAP 2010 equipment (Micromeritics, USA). Other investigated samples (S-2 to S-10) were measured only in the range of relative pressure of nitrogen of 0.01-0.30. Prior to the adsorption isotherm measurement, the samples were degassed at 300 °C under vacuum overnight. The specific surface area was calculated following BET method. The surface vanadium density (V nm^{-2}) was calculated according to equation in Ref. [13].

The UV-vis diffuse reflectance spectra of diluted and subsequently dehydrated samples were measured using Cintra 303 spectrometer (GBC Scientific Equipment, Australia) equipped with a Spectralon-coated integrating sphere using a Spectralon coated discs as a standard. The spectra were recorded in the range of the wavelengths of 190-850 nm. The samples were diluted by the pure silica (Fumed silica, Aldrich) in the ratio 1:100 in order to obtain better resolution of individual bands and the linear dependence of spectral area on the concentration of vanadium (additional details are available in [25]). Dehydration of vanadium-based catalysts was carried out in the static atmosphere of oxygen at 450 °C for 60 min and subsequently the samples were cooled down to 250 °C, evacuated and transferred

into the quartz optical cuvette 5 mm thick and sealed under vacuum. This procedure guaranteed complete dehydration (independently checked by measurement of overtones of OH group vibration on UV-vis-NIR spectrometer) and defined oxidation state of vanadium for all catalysts. For additional details see Ref. [25]. The obtained reflectance spectra were transformed into the dependencies of Kubelka-Munk function $F(R_\infty)$ according to [26].

Redox behavior of VO_x surface species and the accessibility of all vanadium by chemicals agents was investigated by the temperature programmed reduction by hydrogen (H_2-TPR) using the AutoChem 2920 (Micromeritics, USA). A 150 mg of sample in a quartz U-tube microreactor was oxidized in oxygen flow at 450°C (2 hours) prior to the TPR measurement. The reduction was carried out from 25°C to 900°C with a temperature gradient of 10°C/min in flow of reducing gas (5 vol. % H_2 in Ar). The changes of hydrogen concentration were monitored by the TCD detector and simultaneously hydrogen consumption and water formation were also detected by a quadrupole mass spectrometer OmniStar^{TM} GDS 300 (Pfeiffer vacuum, Germany).

2.3 Catalytic tests in ODH and ODH/DH of n-butane

The *n*-butane dehydrogenation (*n*C_4-DH) reaction was carried out in a glass plug-flow fixed-bed reactor at atmospheric pressure and 540 °C in the kinetic region (independently checked) and under steady-state conditions of reaction. The activity and selectivity of catalysts were tested in the dependence on contact times in the range of 0.03-0.24 g_{cat} s cm^{-3}. The load of catalyst (25, 50, 100 or 200 mg) for attaining of particular contact times (grains of 0.25-0.5 mm) was mixed with 3 cm^3 of inert SiC in order to avoid local overheating and to minimize the dead volume of the reactor in the hot zone. All catalysts were pretreated in a flow of oxygen at 450 °C for 2 hours before each reaction run. The concentration of oxygen in the input feed was varied from 5 to 0.1 vol.% at constant amount of *n*-butane (5 vol.%) and the rest was helium. The total constant flow was 6 dm^3 h^{-1} STP. The input feed and the

products were analyzed by on-line connected gas-chromatograph (CHROM 10, Labio, Czech Rep.) using a 1010 Carboxen (Supelco) column for O_2, CO, CO_2, H_2 and a GS-Alumina (Agilent) for *1*-butene, *cis-2*-butene, *trans-2*-butene, butadiene, propene, propane, ethene, ethane and methane connected to TCD and FID detector, respectively. The feed conversion, selectivity to products, turn-over-frequency (TOF) and productivity were calculated based on mass balance according to equations mentioned in Ref [13, 27]. In the case of TOF calculation, only vanadium species with T_d coordination were taken like the active species because most of vanadium particles in V_2O_5 crystallites is not able to participate in ODH of *n*-butane what is confirmed by previously published low activity of these materials [13, 28].

3 Results and discussion

3.1 Characterization of catalysts

The two representative SEM images of the bare support (HMS) and of the sample with the highest concentration of vanadium (S-12) are presented in the Figure 1. Both samples exhibit similar morphology of particles and at the same time no significant differences in particle size distribution were observed in individual samples. It is evident that the morphology was preserved even after the impregnation with the highest amount of vanadium (12 wt. %). Typical orthorhombic V_2O_5 needles were not observed in any sample and no V_2O_5 clusters were detected in SEM-EDX mapping of V content (pictures are not show here for sake of brevity). The concentration of vanadium was distributed homogeneously in all parts of catalyst grains even at the highest vanadium concentration.

Figure 2 shows the powder XRD patterns for pure HMS and V-HMS catalysts in the 2θ range of 2-40°. The region of 2θ value higher than 40° contains no significant signal hence it is not shown here. The patterns show characteristic sharp low-angle diffraction peak at 2θ = 2.1-2.2° corresponding to a d_{100} diffraction typical for hexagonal lattice structure of

mesoporous materials [24, 29] and the broad low-intensity peak in range of 15-35°. Similar patterns were frequently reported for hexagonal mesoporous materials in the literature [13, 29-30]. With rise in VO_X loading the d_{100} peak weakens in intensity and gradually disappears which is the result of the partial blocking of mesopores by VO_X and the decline in long-range order of hexagonal ordered structure [31]. Reflections characteristic for the V_2O_5 crystallites were detected only for samples with vanadium concentration of 8 wt.% of V and more (S-8, S-10 and S-12) and it is represented by three main reflections at 15.4°, 20.2° and 26.1° in the XRD pattern [13, 31-32]. These results are in good agreement with previously published XRD patterns of similar materials [14, 22, 29, 33] but a little in contradiction with our results obtained from DR UV-vis spectroscopy (it will be discussed below), where traces of V_2O_5 crystallites were detected at S-6 sample because presence of spectral bands below 3 eV is ascribed to species with octahedral (O_h) coordination [25], see Figure 3. It is probably due to the very well known limit of XRD. The clear diffraction peaks are observed only when the sample possesses individual phase with sufficient long-range order [34-35].

The specific surface areas determined from adsorption isotherm by BET method for pure HMS and catalysts are summarized in Table 1. The HMS based materials follow the isotherm of type IV (according to IUPAC classification) with narrow hysteresis loop of type H4 which indicates mesoporous character of solids and in this case it is combination of micro- and mesoporous system of channels [36-38]. The average pore diameter of pure HMS support was 6.8 nm with the total pore volume of 0.56 $cm^3\ g^{-1}$ and specific surface BET are area of 830 $m^2\ g^{-1}$. With increasing vanadium loading, the surface area systematically decreases to 70 $m^2\ g^{-1}$ for S-10 sample and after reaching this value it remains at an approximately constant value. These values are in a good agreement with data published previously for this type of materials with similar vanadium content [13-14, 29, 39-40] and they indicate that the VO_X species are located inside the channel system on the inner walls of mesoporous matrix or

deposition of vanadium oxo-species and small V_2O_5 oxide clusters close to pores mouth which block these pores and it leads to decrease of pore volume [31, 41-42]. Moreover, this behavior can be attributed to partial destruction of the framework which was evidenced by TEM for high concentration of vanadium in samples [29, 43].

The surface vanadium density (V atoms per nm^2) represents a parameter that allows comparison of catalysts in a wide range of concentrations and surface areas [44]. On the basis of its value this allows us to predict type of VO_X particles on the surface as well. The systematic study of Wachs's group led to a conclusion that oxide microcrystallites appeared above monolayer coverage, when all the reactive hydroxyls of the support have been titrated [45-46]. Monolayer coverage on silica is significantly lower (about 0.7 V nm^{-2}) in comparison with other supports like alumina, titania and zirconia (about 7–8 V nm^{-2}) [45]. Surface vanadium density of our samples ranges from 0.3 to 24.3 V nm^{-2} therefore presence of oligomeric T_d- and O_h-coordinated VO_X species is reasonable and expectable and it supports conclusions obtained from another characterization techniques such as DR UV-vis and XRD.

The DR UV-Vis spectra of dehydrated samples measured in the range of 1.45–6.5 eV (850–190 nm) are presented in the Figure 3 for all prepared vanadium samples. The parent HMS support exhibited only very low intensity spectrum without distinct signals [25] and therefore is not reported here. Spectra of VO_X-HMS catalysts consist of several ligand to metal charge-transfer (LMCT) transitions of the $O \rightarrow V^{+V}$ type or of the d-d transitions of V^{+IV} [47]. The d–d absorption bands characteristic for the V^{+IV} in the region of 1.55 – 2.07 eV [48] were not observed in our spectra and this fact confirms that all vanadium is presented in oxidation state V^{+V} after pretreatment procedure. The spectra with high concentration of vanadium exhibit absorption bands in the region of 2-3 eV and they are attributed to the presence of 3D-octahedrally coordinated (group of symmetry O_h) bulk-like VO_X units [25, 49]. The absorption bands above 3 eV belong to the ligand to metal charge transfers of

tetrahedrally coordinated (T_d) VO_X species (group of symmetry T_d). We can distinguish two main types of T_d coordinated units: (i) isolated monomeric VO_4 units and (ii) small VO_X polymeric aggregates with V-O-V bonds [25, 36, 49]. For quantitative analysis of all three types of surface vanadium complexes, the spectra were deconvoluted into individual bands. Mathematical parameters used in deconvolution procedure of the spectra were taken from systematic study analyzing wide set of VO_X-HMS samples recently published by our group [25]. The band with position of the maximum approximately at 4 eV can be attributed to T_d oligomeric species [50-51]. The band at ca 5.9 eV belongs to T_d-monomeric species [50-52] and the band with maximum at 5 eV is linear combination of the bands ascribed to both the T_d-monomeric and the T_d-oligomeric species. Relative amount of individual VO_X species on the surface was determined from area of corresponding bands and results are given in the Table 1. The low concentrated samples contain only T_d-coordinated VO_X species. The highest relative abundance of monomeric T_d-coordinated units (33 rel.%) can be found in S-2 with the lowest vanadium content, while relative population of oligomeric T_d-coordinated VO_X species is almost constant (*ca.* 75 rel. %). Population of monomeric species decreases with increasing vanadium content from 33 rel. % to 6 rel. % and simultaneously the population of octahedrally coordinated species increases from zero to 27 rel. %.

H_2-TPR curves were measured to determine the scale dispersion and type of the present active species. The obtained TPR profiles are depicted in the Figure 4 and results of their analysis are summarized in the Table 1. It should be noted that parent supports exhibited no reduction peaks and therefore they are not reported here for the sake of brevity. TPR curves of all samples exhibit only one reduction peak in the temperature range from 440 to 920 °C. Maximum of the reduction peak shifts to higher temperature with increasing vanadium content from 589 to 672 °C. In addition, the reduction peak becomes broader with increasing vanadium content. These effects could be explained in two ways: (i) either this shift can be

ascribed to the kinetics or the thermodynamics of the process of VO_X reduction and it is related to the changes in H_2 to surface vanadium ratio or to ratio of generated H_2O to H_2 during the reduction process with the increasing vanadium loading [53-55] or (ii) due to the gradual formation of VO_X units with different degree of polymerization and/or different structure (T_d, O_h units) [13, 31, 56-57]. The overall hydrogen consumption is proportional to the concentration of vanadium and at the same time corresponds to change of oxidation state during the reduction process. The change of oxidation state varies from 1.7 to 2 electrons per vanadium atom (see Table 1) and it indicates a quantitative reduction of V^{+V} to V^{+III} [13].

3.2 Catalytic tests

Oxidative dehydrogenation of *n*-butane under oxygen rich and oxygen lean conditions was studied at 540°C at various contact times implemented by changes of catalysts weight. The main reaction products identified in the reaction mixture were, 1-butene (1-C_4), *cis*- and *trans*-2-butene (*c*-C_4 and *t*-C_4), 1,3-butadiene (1,3-C_4), methane (C_1), ethane and ethene (C_2), propane and propene (C_3) and carbon oxides (CO and CO_2). The carbon balance was 95±3 % in all the catalytic tests. Under oxygen lean conditions (*n*-C_4/O_2 > 5) we can detect small amount of hydrogen which indicates the contribution of classical dehydrogenation reaction to catalysts activity. Next evidence of presence of DH reaction is the fact that the selectivity to C_4-deh. products (1-C_4, *c*-C_4, *t*-C_4 and 1,3-C_4) is higher than the corresponding oxygen consumption. The extent of dehydrogenation reaction mechanism under lean oxygen conditions (0.1 vol. % of O_2) varies from 70% for S-2 to 30% for S-12 of total catalytic activity and it will be discussed in more detail later.

The activity of bare HMS was measured under the same conditions (540°C and different C_4/O_2 ratio) to check reactivity of neat support. The detected conversion of n-butane was only about 0.5% and selectivity to C4-deh. products was in all cases about 70%. The constant value of conversion and selectivity could be an evidence that this is a reaction in

homogeneous phase as was published in Ref. [58]. However, this conversion is remarkably lower in comparison to the conversions reached over all tested catalysts and hence it will not be further discussed.

One of the main disadvantages of non-oxidative dehydrogenation is fast decline in activity due to carbon deposits on the catalysts surface [19, 59-60] and therefore it is very important investigate the stability of materials under reaction conditions with time on stream. Figure 5 shows the *n*-butane conversion and selectivity to C_4-deh. products over the most active sample S-6 over 14 hours on-stream with *n*-C_4/O_2 ratio 50 (0.1 vol.% of O_2 in input feed and W/F 0.24 g_{cat} s cm^{-3}). The conversion of *n*-butane slightly decreased during this time from its maximum value of *ca* 8 % to *ca* 6 % (*i.e.* decrease of 30 rel.%), while the selectivity to C_4-deh. remained at constant value *ca* 92%. Such relatively stable operation under low oxygen conditions is comparable with stability of similar materials in ODH of *n*-butane and propane [14]. High stability of the catalyst is caused by the high selectivity of VO_X active species and also due to burning of potential coke deposits by oxygen in the stream. All data which will be subsequently discussed in this paper were obtained after 3 hours on-stream.

The dependence of S *vs.* X obtained for all loads of catalyst and O_2 concentrations over the S-4 sample are presented in Figure 6 (other samples are not shown for sake of brevity). The highest conversion values were reached for experiments carried out with 5 vol. % of O_2 in input reaction mixture and subsequent decrease of oxygen amount caused the conversion values to decrease. This effect can be ascribed to the fact that according to the Ref. [10] the ODH process has a significantly higher reaction rate than DH reaction which takes place mainly under oxygen lean conditions.

It is clearly perceptible that selectivity to C_4 products depends only slightly on the conversion for experiments with low O_2 concentration and low conversion degree value and indicates that under these conditions the C_4 products are formed *via* a parallel reaction

pathway either by ODH and/or by DH reaction. The limiting of C_4-deh. selectivity value at zero conversion degree depends on the initial amount of O_2 in the reaction mixture and indicates that at least a part of n-butane can be directly overoxidized to carbon oxides in one step at certain active sites by process accompanying the ODH reaction. On the other hand the decrease of O_2 amount in the reaction mixture leads to increase of selectivity to C_4-deh. products up to values of *ca.* 95% obtained for *n*-C_4/O_2 ratio 50. This effect means that the DH reaction responsible for larger part of catalytic activity under these conditions is significantly more selective process in comparison with ODH reaction in agreement with Refs. [1-2, 10].

The selectivity to C_4-deh. products started to decrease when the higher degree of *n*-butane conversion over catalyst samples reached a certain value (in Figure 6 denoted by dashed line), either by increase of O_2 amount in the reaction mixture or by the increase of catalyst load. This effect means that the consecutive over-oxidation of C_4 ODH/DH began to participate more significantly in reaction pathway of studied reaction [10]. Common part of the S ~ X dependences for 2, 3 and 5 % of O_2 in reaction mixture suggests that this dashed line represents the limiting selectivity which can be obtained over particular catalyst at given value of conversion degree. The Figure 7 shows the dependence of selectivity to C_4-deh. products on the conversion degree obtained for various amount of O_2 in the reaction mixture over maximum load of catalysts (200 mg). Dependencies in Figure 7 hence correspond to these limits of S *vs*. X for whole set of tested catalysts.

The C_4-deh. selectivity values are always the highest at certain conversion degree for samples with the lowest vanadium content and decrease with the increasing vanadium content. Additionally, the selectivity to the C_4-deh. products starts to decrease after reaching of certain *ca* 4-6% limiting conversion degree for samples with low vanadium concentration. This effect is an evidence that at least for these samples the DH reaction significantly

participates in the C_4-deh. products formation when the oxygen concentration in the reaction mixture limits to zero (*n*-$C_4/O_2 > 5$).

The earlier start of participation of consecutive alkene oxidation over S-8 – S-12 sample in comparison with S-2 – S-6 samples is most likely caused by the presence of substantial amount of highly polymerized VO_X species in samples with higher vanadium concentration which do not activate *n*-butane but are active in oxidation of alkenes to products of total combustion.

It is generally known that the catalytic behavior and mainly selectivity of catalysts with different vanadium loading is necessary to compare at the same degree of conversion, especially for parallel-consecutive reaction, such as the ODH/DH reaction of *n*-butane. Therefore Figure 8 and Table 2 show iso-conversion data for four different *n*-C_4/O_2 ratios with 5, 1, 0.5 and 0.1 vol.% of O_2 in the feed, respectively. Due to relatively steep dependence of conversion on *n*-C_4/O_2 ratio, the *n*-butane conversion of 13 % is taken as iso-conversion conditions in the case of 5 vol.% in the feed. For 1 vol.% of O_2 in the feed the data at 6 % of *n*-butane conversion and for the 0.1 and 0.5 vol.% of O_2 in the feed, we take data at 3 % conversion of *n*-butane were taken.

The activity of catalysts could be expressed by so called Turn-Over–Frequency (TOF), describing the average number of catalytic cycles at one active centre per time unit (in our case hour). In our case only vanadium species with T_d coordination could be taken like active species because bulk V_2O_5 with O_h structure is almost inactive in ODH of n-butane [13]. The TOF value exhibits similar dependence on the concentration of vanadium for all *n*-C_4/O_2 ratios as shown in the Figure 8. The three low concentrated samples (S-2 – S-6) exhibit approximately constant value of TOF. After reaching vanadium concentration of *ca* 6 wt. % rapid decrease of TOF to low value occurs (for high *n*-C_4/O_2 ratio it is almost zero). Decrease of TOF value clearly shows that with subsequent increase of vanadium content the

significantly less active (polymeric species) or non-active (bulk V_2O_5) species in ODH of *n*-butane are generated.

The selectivity to C_4-deh. products starts to decrease after reaching *ca* 6 wt.% of vanadium on the surface for all *n*-C_4/O_2 ratio. This effect can be ascribed to increased population of highly polymerized VO_X species and mainly to presence of VO_X species with O_h coordination which serve as "oxygen storage" and can cause the immediate over-oxidation of alkenes formed at active site without necessity of a consecutive desorption and readsoption reaction step. Moreover the decrease in selectivity is more pronounced for low *n*-C_4/O_2 ratio where the influence of ODH (less selective than DH [1]) is more evident as it was already discussed above. The decrease in iso-conversion C_4-deh. selectivity is accompanied by increase in selectivity to CO_X with CO/CO_2 ratio of 1.6 (± 0.2) under all feed compositions.

From above discussed results we can conclude that the monomeric VO_X units should be taken as the most active and selective species not only in ODH of *n*-butane as it was reported previously [13] but in DH of *n*-butane as well. Determination of monomeric units as the most active species in DH of *n*-butane was reported previously by McGregor et al. [19], however, they attributed low selectivity to these species.

4 Conclusions

For the first time, we report a highly selective (selectivity to C_4-deh. products over 90% at conversion 8.5-6%) and for a relatively long time stable (at least 14 hours on stream) *n*-butane dehydrogenation over vanadium oxide species supported on HMS under oxygen-lean conditions. From data obtained on samples with various population and different coordination of VO_X species we can conclude that isolated monomeric VO_X units play the role of the most active and selective catalytic centre in both ODH and DH reaction, respectively. Concentration of these units achieves the highest concentration around 5 wt. % of vanadium on the surface and these samples exhibit the highest productivity in

dehydrogenation of *n*-butane. The presence of oligomeric VO_X species is responsible for over-oxidation of *n*-butane and mainly of butenes even in oxygen-lean conditions.

Acknowledgements

A financial support of the Grant Agency of the Czech Republic under the project No. P106/10/0196 is highly acknowledged. We also thank to Peter Priecel for proofreading.

References

1. Cavani F, Ballarini N, Cericola A (2007) Catalysis Today 127: 113
2. Ovsitser O, Schomaecker R, Kondratenko EV, Wolfram T, Trunschke A (2012) Catalysis Today 192: 16
3. Jackson SD, Rugmini S (2007) Journal of Catalysis 251: 59
4. Bhasin MM, McCain JH, Vora BV, Imai T, Pujado PR (2001) Applied Catalysis A General 221: 397
5. Tsikoyiannis JG, Stern DL, Grasselli RK (1999) Journal of Catalysis 184: 77
6. Rase HF (2000) Handbook of Commercial Catalysts. CRC Press, New York
7. Dean JA (1999) Lange´s handbook of chemistry. McGraw-Hill Inc., New York
8. Chaar MA, Patel D, Kung MC, Kung HH (1987) Journal of Catalysis 105: 483
9. Madeira LM, Portela MF (2002) Catalysis Reviews-Science and Engineering 44: 247
10. Ovsitser O, Kondratenko EV (2010) Chemical Communications 46: 4974
11. Grasselli RK, Stern DL, Tsikoyiannis JG (2000) In: Corma A, Melo FV, Mendioroz S, Fierro JLG (eds) Studies in Surface Science and Catalysis, vol Volume 130. Elsevier p 773
12. Waku T, Biscardi JA, Iglesia E (2004) Journal of Catalysis 222: 481
13. Setnička M, Bulánek R, Čapek L, Čičmanec P (2011) Journal of Molecular Catalysis A Chemical 344: 1
14. Bulánek R, Kalužova A, Setnička M, Zukal A, Čičmanec P, Mayerová J (2012) Catalysis Today 179: 149
15. Čapek L, Adam J, Grygar T, Bulánek R, Vradman L, Kosova-Kucerová G, Čičmanec P, Knotek P (2008) Applied Catalysis A General 342: 99
16. Blasco T, Nieto JML (1997) Applied Catalysis A General 157: 117
17. Weckhuysen BM, Keller DE (2003) Catalysis Today 78: 25

18. Tian HJ, Ross EI, Wachs IE (2006) Journal of Physical Chemistry B 110: 9593
19. McGregor J, Huang Z, Shiko G, Gladden LF, Stein RS, Duer MJ, Wu Z, Stair PC, Rugmini S, Jackson SD (2009) Catalysis Today 142: 143
20. Harlin ME, Niemi VM, Krause AOI, Weckhuysen BM (2001) Journal of Catalysis 203: 242
21. Xu YB, Lu JY, Zhong M, Wang JD (2009) Journal of Natural Gas Chemistry 18: 88
22. Bulánek R, Čičmanec P, Sheng-Yang H, Knotek P, Čapek L, Setnička M (2012) Applied Catalysis A General
23. Kung HH (1994) Advances in Catalysis (Advances in Catalysis), vol 40. Academic Press Inc, San Diego p 1
24. Tanev PT, Pinnavaia TJ (1995) Science 267: 865
25. Bulánek R, Čapek L, Setnička M, Čičmanec P (2011) Journal of Physical Chemistry C 115: 12430
26. Kubelka P, Munk FZ (1931) Technical Physics 12: 593
27. Sachtler WMH, Boer NHD (1964) Proc. 3rd Int. Congr. Catalysis. North-Holland Publishing Company, Amsterdam p 8
28. Owens L, Kung HH (1993) Journal of Catalysis 144: 202
29. Karakoulia SA, Triantafyllidis KS, Lemonidou AA (2008) Microporous and Mesoporous Materials 110: 157
30. Chen C, Zhang QH, Gao J, Zhang W, Xu J (2009) Journal of Nanoscience and Nanotechnology 9: 1589
31. Liu W, Lai SY, Dai HX, Wang SJ, Sun HZ, Au CT (2007) Catalysis Letters 113: 147
32. Wang WJ, Lin HY, Chen YW (2007) Journal of Porous Materials 14: 137
33. Kondratenko EV, Cherian M, Baerns M, Su DS, Schloegl R, Wang X, Wachs IE (2005) Journal of Catalysis 234: 131

34. Niemantsverdriet JW (2007) Spectroscopy in Catalysis. Wiley-VCH, Weinheim
35. Sarsfield BA, M. Davidovich, Desikan S, Fakes M, Futernik S, Hilden JL, Tan JS, Yin S, Young G, Vakkalagadda B, Volk B (2006) Denver X-ray Conference (Advances in X-ray Analysis), vol 49. JCPDS, Denver p 322
36. Knotek P, Čapek L, Bulánek R, Adam J (2007) Topics in Catalysis 45: 51
37. Čejka J, Corma A, Bekkum Hv, Schüth F (2007) Introduction to zeolite science and practice Elsevier
38. Lowell S, Shields JE, Thomas MA, Thommes M (2004) Characterization porous solids and powders: surface area, pore size and density. Kluwer Academic Publishers, Dordrecht
39. Čapek L, Bulánek R, Adam J, Smoláková L, Sheng-Yang H, Čičmanec P (2009) Catalysis Today 141: 282
40. Zhou R, Cao Y, Yan SR, Deng JF, Liao YY, Hong BF (2001) Catalysis Letters 75: 107
41. Zukal A, Šiklová H, Čejka J (2008) Langmuir 24: 9837
42. Hess C, Hoefelmeyer JD, Tilley TD (2004) Journal of Physical Chemistry B 108: 9703
43. Karakoulia SA, Triantafyllidis KS, Tsilomelekis G, Boghosian S, Lemonidou AA (2009) Catalysis Today 141: 245
44. Centi G (1996) Applied Catalysis A General 147: 267
45. Wachs IE, Weckhuysen BM (1997) Applied Catalysis A General 157: 67
46. Wachs IE (1996) Catalysis Today 27: 437
47. Keller DE, Visser T, Soulimani F, Koningsberger DC, Weckhuysen BM (2007) Vibrational Spectroscopy 43: 140

48. Mathieu M, Van Der Voort P, Weckhuysen BM, Rao RR, Catana G, Schoonheydt RA, Vansant EF (2001) Journal of Physical Chemistry B 105: 3393

49. Solsona B, Blasco T, Nieto JML, Pena ML, Rey F, Vidal-Moya A (2001) Journal of Catalysis 203: 443

50. Gao F, Zhang YH, Wan HQ, Kong Y, Wu XC, Dong L, Li BQ, Chen Y (2008) Microporous and Mesoporous Materials 110: 508

51. Schramlmarth M, Wokaun A, Pohl M, Krauss HL (1991) Journal of the Chemical Society - Faraday Transactions 87: 2635

52. Catana G, Rao RR, Weckhuysen BM, Van Der Voort P, Vansant E, Schoonheydt RA (1998) Journal of Physical Chemistry B 102: 8005

53. Hurst NW, Gentry SJ, Jones A, McNicol BD (1982) Catalysis Reviews-Science and Engineering 24: 233

54. Kissinger HE (1957) Analytical Chemistry 29: 1702

55. Du G, Lim S, Pinault M, Wang C, Fang F, Pfefferle L, Haller GL (2008) Journal of Catalysis 253: 74

56. Kanervo JM, Harlin ME, Krause AOI, Banares MA (2003) Catalysis Today 78: 171

57. Kustrowski P, Segura Y, Chmielarz L, Surman J, Dziembaj R, Cool P, Vansant EF (2006) Catalysis Today 114: 307

58. Cavani F, Trifiro F (1999) Catalysis Today 51: 561

59. Vrieland GE, Murchison CB (1996) Applied Catalysis A General 134: 101

60. Harlin ME, Backman LB, Krause AOI, Jylha OJT (1999) Journal of Catalysis 183: 300

Figures caption, tables and figures

Figure 1 SEM images of bare HMS support (A) and a sample S-12 (B) with the highest vanadium content.

Figure 2 X-ray diffraction patterns for bare support and all V-HMS catalysts.

Figure 3 Diffuse reflectance UV-Vis spectra of diluted and dehydrated V-HMS catalysts.

Figure 4 H_2-TPR patterns for all V-HMS catalysts.

Figure 5 *n*-Butane conversion (black circle) and C_4-deh. selectivity (red triangle) as a function of time-on-stream at 540°C over S-6 catalysts (W/F 0.24 g s ml^{-1}). Composition of reaction mixture: 5 vol.% of *n*-butane, 0.1 vol.% of O_2 and rest He**.**

Figure 6 Selectivity to C_4-deh. products as a function of conversion obtained at different contact time (0.03, 0.06, 0.12 and0.24 g_{cat} s cm^{-3}) and different oxygen content in reaction mixture (different colors and shapes) for representative S-4 catalyst at 540 °C with total flow 6 dm^3 h^{-1} STP and 5 vol.% of *n*-butane in feed.

Figure 7 Dependence of selectivity to C_4-deh. products on conversion at different oxygen content in reaction mixture for 200 mg of catalyst**.**

Figure 8 Isoconversion of the turn-over-frequencies (red circle) and selectivity (stacked bar) obtained at 540 °C and different *n*-C_4/O_2 ratio. For *n*-C_4/O_2 = 1 are data taken at 13% of *n*-butane conversion, for *n*-C_4/O_2 = 5 at 6% and for *n*-C_4/O_2 = 10 and 50 at 3% of *n*-butane conversion.

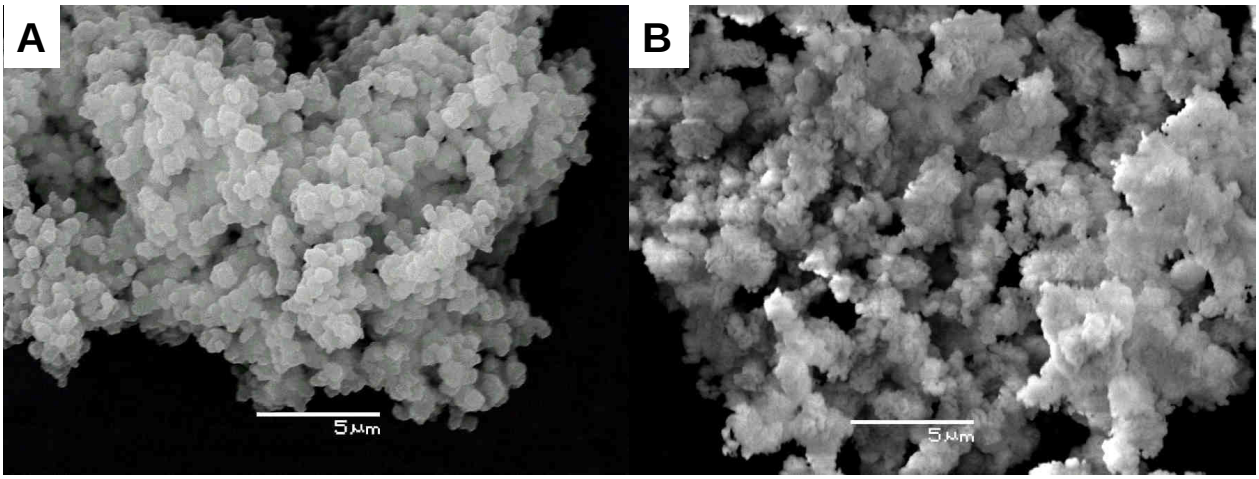

Figure 1

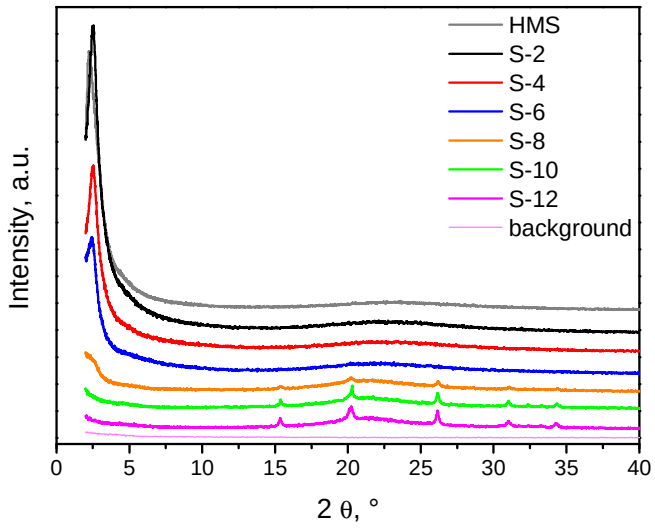
HMS
S-2
S-4
S-6
S-8
S-10
S-12
background
Intensity, a.u.
0
5
10
15
20
25
30
35
40
2 θ, °

Figure 2

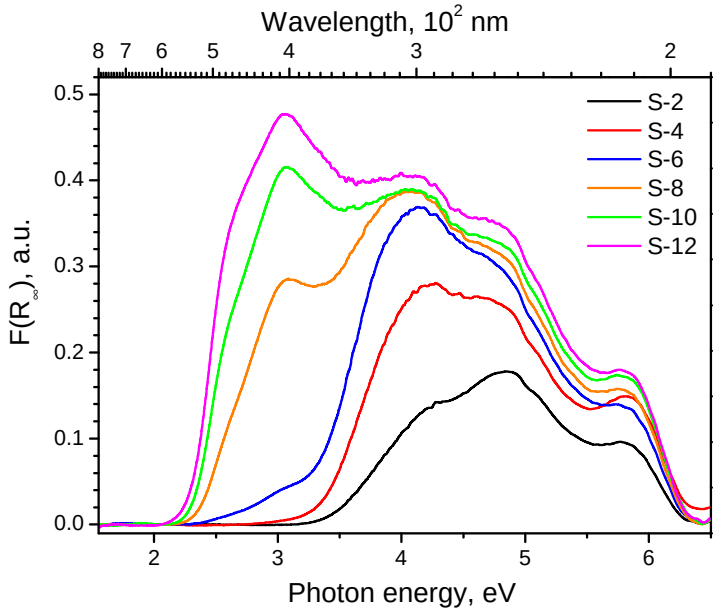
Wavelength, 10^2 nm
8 7 6 5 4 3 2
0.5
0.4
0.3
0.2
0.1
0.0
F(R∞), a.u.
2 3 4 5 6
Photon energy, eV
S-2
S-4
S-6
S-8
S-10
S-12

Figure 3

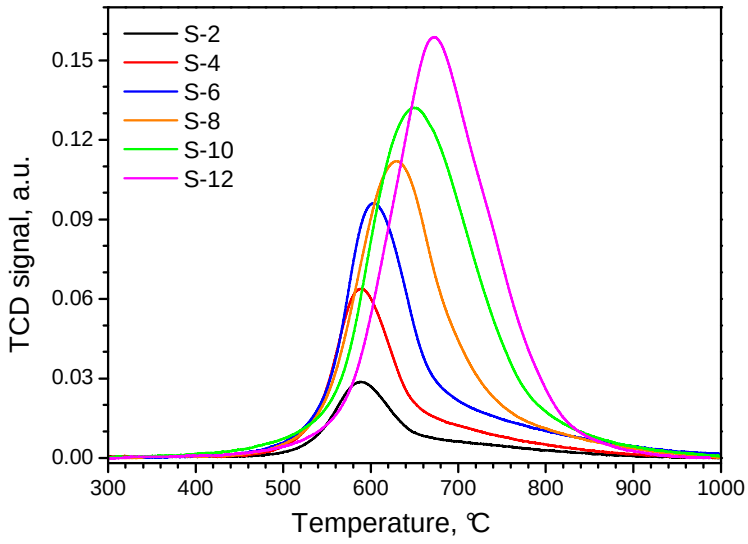
S-2
S-4
S-6
S-8
S-10
S-12
TCD signal, a.u.
0.00
0.03
0.06
0.09
0.12
0.15
300
400
500
600
700
800
900
1000
Temperature, ℃

Figure 4

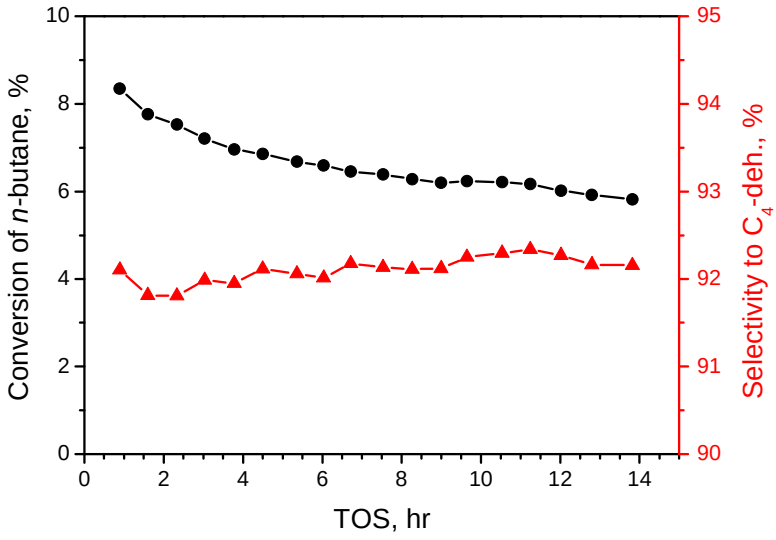
Conversion of n-butane, %
Selectivity to C4-deh., %
TOS, hr
0
2
4
6
8
10
12
14
90
91
92
93
94
95

Figure 5

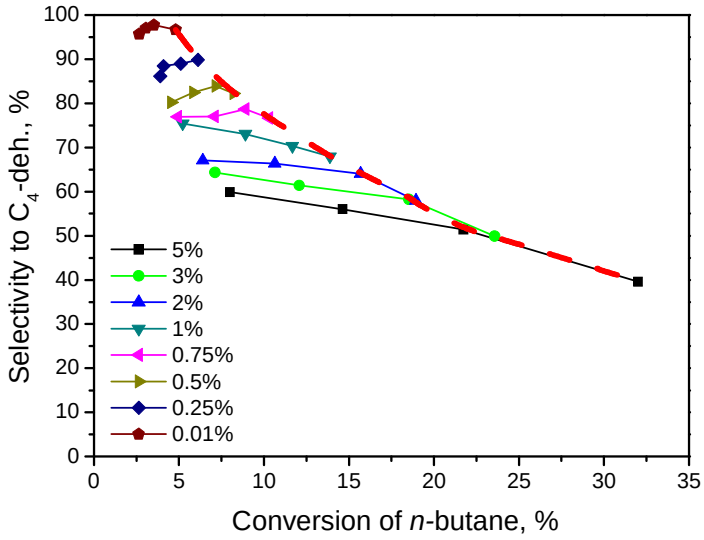
Selectivity to C4-deh., %
Conversion of n-butane, %
5%
3%
2%
1%
0.75%
0.5%
0.25%
0.01%
0
10
20
30
40
50
60
70
80
90
100
0
5
10
15
20
25
30
35

Figure 6

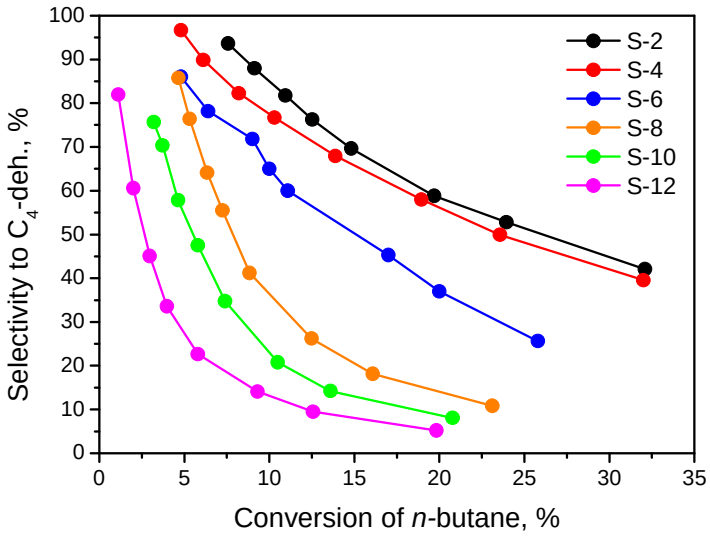
Selectivity to C4-deh., %
Conversion of n-butane, %
S-2
S-4
S-6
S-8
S-10
S-12
0
10
20
30
40
50
60
70
80
90
100
0
5
10
15
20
25
30
35

Figure 7

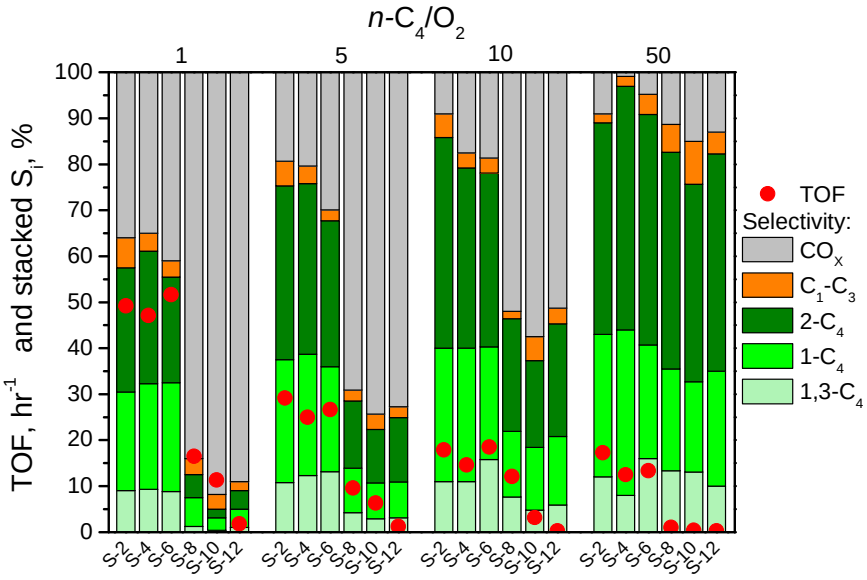
n-C4/O2
1
5
10
50
TOF, hr-1 and stacked Si, %
TOF
Selectivity:
COX
C1-C3
2-C4
1-C4
1,3-C4
S-2
S-4
S-6
S-8
S-10
S-12

Figure 8

Table 1
Chemical composition and results of physico-chemical characterization of investigated materials

sample name	V[a], wt.%	S_{BET}, $m^2.g^{-1}$	VO_X[b], nm^{-2}	Relative population of VO_X complexes			T_{max}[c], °C	Δe[d]
				O_h	T_d^{oligo}	T_d^{mono}		
HMS		830						
S-2	2	760	0.3	0.00	0.67	0.33	589	1.7
S-4	4	645	0.7	0.00	0.70	0.30	590	1.8
S-6	6	450	1.6	0.02	0.81	0.17	603	2.0
S-8	8	225	4.2	0.15	0.77	0.08	629	1.9
S-10	10	70	17.5	0.23	0.70	0.08	650	2.0
S-12	12	60	24.3	0.27	0.67	0.06	672	2.0

[a] Vanadium content determined by XRF method (error: ±0.2 wt.%)

[b] VO_X surface density (VO_X nm^{-2})

[c] Position of maxima of H_2-TPR profile

[d] Average change in oxidation state of vanadium during H_2-TPR

Table 2
Results of catalytic tests in dehydrogenation of *n*-butane at 540°C and iso-conversion of *n*-butane at different C_4/O_2 ratio with 5 vol.% of C_4H_{10} and total flow rate of 100 cm^3 min^{-1}.

Sample name[a]	C_4/O_2 ratio	Conversion, %		Selectivity, %						TOF hr^{-1}
		C_4H_{10}	O_2	1-C_4	2-C_4	1,3-C_4	C_1-C_3[b]	CO_2	$\sum C_4$[c]	
S-2	1	13	30	22	27	9	7	36	58	49
S-4		13	33	23	29	9	4	35	61	47
S-6		13	30	21	22	9	4	45	51	52
S-8		13	56	6	5	1	3	84	13	16
S-10		13	57	3	2	0	3	92	5	12
S-12		13	64	4	4	1	2	89	9	2
S-2	5	6	40	27	38	11	5	19	75	29
S-4		6	45	26	37	12	4	20	76	25
S-6		6	86	23	32	13	2	30	68	27
S-8		6	100	10	15	4	2	69	29	10
S-10		6	100	8	12	3	3	74	22	6
S-12		6	100	8	14	3	2	73	25	2
S-2	10	3	30	29	45	11	5	9	85	18
S-4		3	47	29	39	11	3	18	79	15
S-6		3	100	25	38	16	3	19	78	19
S-8		3	100	14	25	8	2	52	46	12
S-10		3	100	14	19	5	5	58	37	3
S-12		3	100	15	24	6	3	51	45	< 1
S-2	50	3	64	31	46	12	2	9	89	17
S-4		3	100	36	53	8	2	1	97	12
S-6		3	100	25	50	16	4	5	91	13
S-8		3	100	22	47	13	6	11	83	1
S-10		3	100	20	43	13	9	15	76	< 1
S-12		3	100	25	47	10	5	13	82	< 1

[a] The x in the sample name (S-x) indicates the vanadium content in wt.%

[b] C_1-C_3 = sum of C_1-C_3 hydrocarbons

[c] $\sum C_4$ = sum of C_4 alkene selectivity